Acidity Order of Selected Brønsted Acids in the Gas Phase at 300°K

Diethard K. Bohme,*[1a] Edward Lee-Ruff,[1a] and L. Brewster Young[1b]

Contribution from the Department of Chemistry, York University, Downsview, Ontario, Canada, and the Mobil Chemical Company, Edison, New Jersey 08817. Received July 29, 1971

Abstract: A study of the kinetics of proton-transfer reactions of the type $A^- + BH \rightleftharpoons B^- + AH$ proceeding in the gas phase at 300°K has led to information regarding the difference in acid strength of the acids AH and BH in the gas phase. Forward and reverse rate constants for proton transfer were measured using the flowing afterglow technique and then employed to calculate limits to, or absolute values for, the thermodynamic equilibrium constant which is a direct measure of the difference in pK_a (gas) for the acids AH and BH. The kinetic data for 58 proton-transfer reactions involving various oxygen and carbon acids led to the following acidity scale: $n\text{-}C_4H_9SH >$ $CH_3NO_2 > C_5H_6 \gtrsim CHCl_3 > CH_3COCH_3 > CH_3CN > CH_2Cl_2, CH_3SOCH_3 \gtrsim C_2H_2, tert\text{-}C_4H_9OH, i\text{-}C_3H_7OH >$ $C_2H_5OH > CH_3OH > C_3H_4, C_6H_5CH(CH_3)_2 > C_6H_5CH_3 > C_3H_6 > H_2O > C_6H_6 > H_2 > NH_3 > C_2H_4, C_6H_{12},$ $(CH_2)_3, CH_4$. A comparison of the gas-phase acidity order with the solution order provided further evidence for the extreme sensitivity of the pK_a of certain acids toward solvation. Several changes in the sign of ΔpK_a in going from the gas phase to solution were identified. The preferred direction of proton transfer displayed a moderately high reactivity in the majority of the proton-transfer reactions investigated. However, in a few cases there was some evidence for steric hindrance toward proton transfer in the gas phase. Finally, the identification of the preferred direction of proton transfer allowed the determination of chemically useful limiting values for the electron affinities of a number of hydrocarbon radicals and proton affinities of a number of organic anions.

Recent experimental innovations have made an increasing number of organic anions available in the gas phase for direct observation and study. Examinations of the modes of generation of these ions and their reaction with organic and inorganic substrates in the gas phase are now leading to hitherto unavailable information on the intrinsic stability and reactivity of these anions. For example, experimental determinations of the kinetics of proton-transfer reactions of the type

$$A^- + BH \underset{\longleftarrow}{\overset{\longrightarrow}{\rightleftharpoons}} B^- + AH \qquad (1)$$
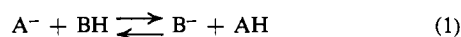
are leading to intrinsic acidity orders which should have an important bearing on reactivity functions measured in solution as well as providing data for identifying intrinsic structure–reactivity patterns for Brønsted acids.[2-4]

In this paper we report the determination of the acidity order of selected Brønsted acids using the flowing afterglow technique. We assert that in the reaction region of a flowing afterglow the acid–base reactions proceed under thermal equilibrium conditions at an operating temperature of 300°K. The determination of the preferred direction of proton transfer under these conditions identifies the sign of the standard free energy change, $\Delta G°_{300}$, in these reactions which, in turn, establishes relative gas-phase acidity.

Experimental Section

Apparatus and Reagents. The experiments were performed in one of the flowing afterglow systems of the National Oceanic and

Atmospheric Administration, Environmental Research Laboratories, Boulder, Colo. Details of the method of operation and data analysis have been thoroughly described elsewhere both with reference to the investigation of thermal energy ion-molecule reactions of interest in the earth's ionosphere,[5] and the novel application of this technique to the study of negative-ion organic chemistry in the gas phase.[4]

The flow system (Figure 1) is a stainless steel tube about 100 cm long with an internal diameter of 8 cm. Helium was used as the carrier gas. A fast helium flow with a velocity in the vicinity of 10^4 cm sec^{-1} is established in the tube by means of a Roots pump backed with a mechanical forepump. With a helium flow of 180 atm cm^3 sec^{-1} and maximum pumping speed, the helium pressure in the tube was typically ca. 0.4 Torr.

Negative ions were generated either directly by electron impact or indirectly by ion-molecule reaction. H^- and NH_2^- ions were produced by the dissociative ionization and dissociative attachment reactions of electrons with NH_3 added upstream from the electron gun (source gas inlet -1). The electron energies were of the order of 30 and 100 eV, respectively. The possible confusion of NH_2^- with O^-, which both have m/e 16 (which is monitored downstream with a quadrupole mass spectrometer), is precluded by the fast reaction of O^- with NH_3 (eq 2) since large amounts (ca. 1 atm cm^3

$$O^- + NH_3 \longrightarrow OH^- + NH_2 \qquad (2)$$
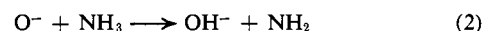
sec^{-1}) of NH_3 were added into the excitation region; reaction 2 has a measured rate constant of 1.2×10^{-9} cm^3 molecule^{-1} sec^{-1} at 295°K.[6] Formation of O^- may result from electron impact on O_2 or other impurities in the excitation region. This mode of production of NH_2^- and H^- ions was invariably accompanied by significant production of OH^- ions. Sources of OH^- ions other than reaction 2 include the fast reactions of H^- and NH_2^- with H_2O impurities in the system (eq 3 and 4).[4b] The generation of anions

$$H^- + H_2O \longrightarrow OH^- + H_2 \qquad (3)$$

$$NH_2^- + H_2O \longrightarrow OH^- + NH_3 \qquad (4)$$
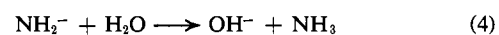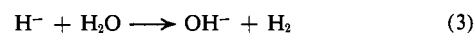
other than NH_2^- and H^- prior to the reaction region was accomplished by ion-molecule reaction. OH^- ions were generated by reaction 2 or the reaction of O^- with saturated or unsaturated hydrocarbon molecules (eq 5).[4a] The phenyl anion, $C_6H_5^-$, was

(1) (a) York University; (b) Mobil Chemical Co.

(2) (a) J. I. Brauman and L. K. Blair, *J. Amer. Chem. Soc.*, **92**, 5986 (1970); (b) *ibid.*, **90**, 5636 (1968); (c) *ibid.*, **91**, 2126 (1969); (d) P. Kriemler and S. E. Buttrill, Jr., *ibid.*, **92**, 1123 (1970).

(3) D. Holtz, J. L. Beauchamp, and J. R. Eyler, *ibid.*, **92**, 7045 (1970).

(4) (a) D. K. Bohme and L. B. Young, *ibid.*, **92**, 3301 (1970); (b) L. B. Young, E. Lee-Ruff, and D. K. Bohme, *Can. J. Chem.*, **49**, 979 (1971); (c) D. K. Bohme, E. Lee-Ruff, and L. B. Young, *J. Amer. Chem. Soc.*, **93**, 4608 (1971).
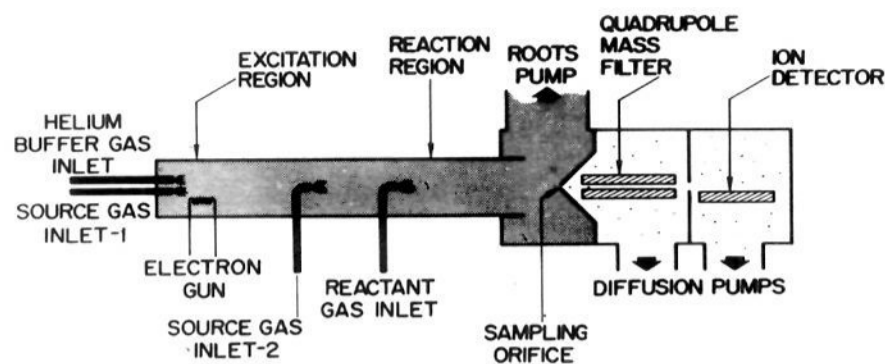
(5) (a) E. E. Ferguson, *Advan. Electron. Electron Phys.*, **24**, 1 (1968); (b) E. E. Ferguson, F. C. Fehsenfeld, and A. L. Schmeltekopf, *Advan. At. Mol. Phys.*, **5**, 1 (1969).

(6) D. K. Bohme and F. C. Fehsenfeld, *Can. J. Chem.*, **47**, 2715 (1969).
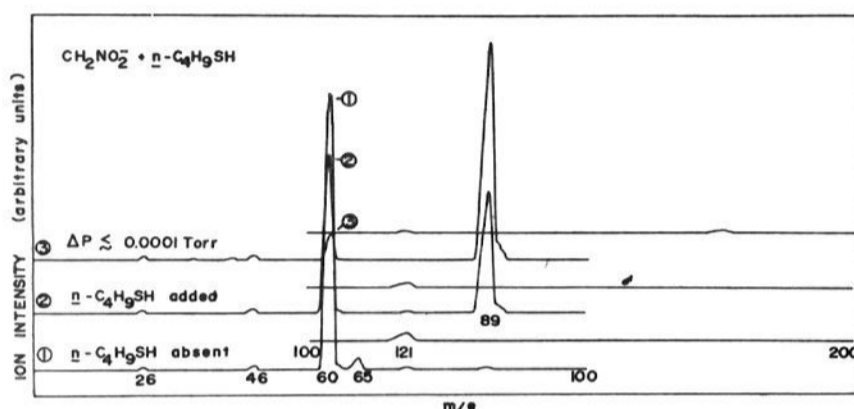
Figure 1. Schematic diagram of the flowing afterglow apparatus.

Figure 2. Spectral scans taken for the reaction of $CH_2NO_2^-$ with *n*-butyl mercaptan proceeding in the gas phase at 300°K.

$$O^- + RH \longrightarrow OH^- + R \qquad (5)$$

generated by the reaction of NH_2^- and H^- with benzene vapor. The generation of the conjugate bases of acids more acidic than H_2O in the gas phase was accomplished by the proton-transfer reaction of NH_2^-, H^-, and OH^- with the corresponding acid. Once the desired anion had been established prior to the reaction region, the desired proton-transfer reaction was investigated by introducing the vapor of the appropriate neutral substrate into the reactant gas inlet. The decline of the ion signal of the desired anion, together with the variation of the ion signals of chemically coupled anions, were then monitored as a function of neutral substrate addition.

It was imperative to add sufficient amounts of neutral gas upstream from the reaction region when the reactant anions were generated by ion–molecule reaction to ensure optimum conversion of the precursor anion such as NH_2^-, H^-, and OH^- to the desired reactant anion prior to the reaction region. Insufficient conversion would lead to declines in the reactant anion signals which would reflect, at least partially, the depletion of the precursor anions. This would be especially serious if the precursor anion reacted rapidly and the reactant anion reacted only slowly with the neutral acid substrate added into the reaction region. Optimum operation often required a ratio of the reactant anion concentration to the precursor anion concentration of at least 100 at the reactant inlet. This was best accomplished with reactions with large equilibrium constants and, in the case where proton-transfer reactions served as the source of reactant anions, by keeping the ratio of the conjugate acid concentration of the reactant anion to the conjugate acid concentration of the precursor anion as large as possible.

The various reactant ions produced in the manner described above were allowed to undergo many thousands of collisions with the helium carrier gas atoms before they entered the reaction region into which the desired neutral substrate was added. In the region following the addition of neutral substrate, characteristic reactions between the anions and the neutral substrate took place (the reaction region was terminated by the sampling orifice of a mass spectrometer). The negative ion composition was then sampled, mass analyzed by means of a quadrupole mass spectrometer, and counted with conventional counting equipment.

The helium carrier gas had a purity of 99.995 mol %; the anhydrous ammonia had a purity of 99.0 mol %. The various organic substrates were reagent grade and ordinary distilled water served as the water source.

Data Acquisition and Analysis. In most of the present experiments, a mass spectrum of the negative ions present in the flowing afterglow at the sampling orifice was recorded over and above the entire mass range dictated by the stoichiometry of the reaction under investigation. Scans were taken both before and after addition of
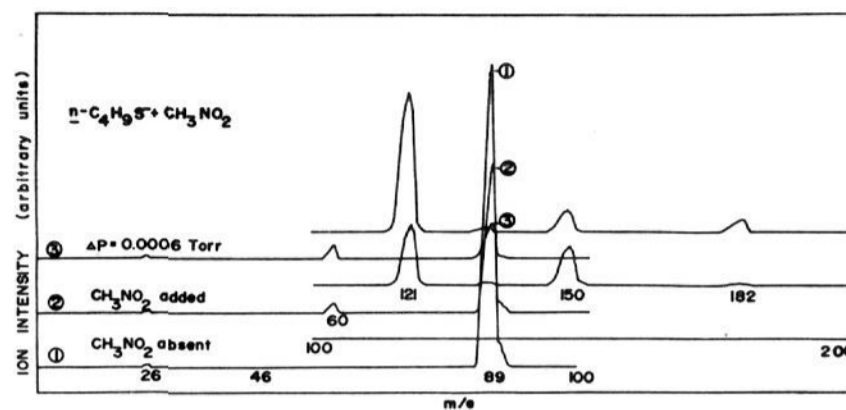

Figure 3. Spectral scans taken for the reaction of *n*-$C_4H_9S^-$ with nitromethane proceeding in the gas phase at 300°K.

neutral substrate into the reaction region. Usually a mass range from m/e 0 to 200 was scanned. These scans allowed an identification of the prinicipal negative ions present both before and after reaction with the neutral substrate. This in turn permitted the identification of chemical coupling by ion–molecule reactions. The variation of the desired anion signal as a function of neutral substrate addition allowed the determination of a value or a limit for the rate constant for the reaction of this anion with the added substrate. This rate constant will correspond to the rate constant for the proton-transfer reaction if the conjugate base of the neutral substrate is the only product ion. If other product ions are observed, the measured rate constant represents an upper limit to the rate constant for the proton-transfer reaction. According to the mass scans taken, all product ions with an intensity of at least 5% of the primary ion should certainly have been observed.

The calculation of a rate constant requires a knowledge of the concentration of the neutral substrate in the reaction region. When the neutral substrate was a stable gas at 300°K, it was monitored quantitatively using the conventional flow measurement technique and the rate constant was determined in the usual manner. When the neutral substrate was a liquid at 300°K, its concentration could not be measured by metering the pure vapor into the flow tube through calibrated flow elements, which is our conventional technique for measuring neutral reactant concentrations. Instead, the concentration of the vapor of the neutral substrate present in the reaction region was measured by monitoring the increase in the total pressure in the reaction region as the vapor of the neutral substrate was bled into it.[7] The smallest partial pressure of the vapor which could be measured in this way was, at best, 0.1 μ. A capacitance manometer with a 10-Torr sensing head served as the pressure measuring device. The accuracy of the rate constants obtained when the concentration of the neutral substrate in the reaction region was measured by metering its flow should be $\pm 30\%$ and the relative accuracy should be $\pm 10\%$. High accuracy is not claimed for the rate constants and the rate constant limits determined by the total pressure increase method. In these cases, the rate constants are considered to be reliable only to within a factor of 2. Such accuracy is nevertheless quite sufficient in the determination of the preferred direction of a reaction.

Results

Table I summarizes the proton-transfer reactions investigated at 300°K. In many cases, both the forward and backward reactions were investigated separately in order to establish unequivocally the preferred direction of proton transfer and thus the sign of the standard free energy change in the proton-transfer reaction at 300°K. For example, the experimental data shown in Figures 2 and 3 were employed to establish the preferred direction of proton transfer between *n*-butyl mercaptan and nitromethane. Figure 2 displays mass spectral scans taken at various extents of the reaction of $CH_2NO_2^-$ with *n*-butyl mercaptan. The addition of nitromethane to a helium afterglow containing NH_2^-, OH^-, and H^- ions resulted in the mass spectrum labeled 1 in Figure 2. The m/e 60 ion is seen to be the dominant ion. Small

(7) F. C. Fehsenfeld, M. Mosesman, and E. E. Ferguson, *J. Chem. Phys.*, **55**, 2115 (1971).

Table I. Summary of Kinetic Data for Acid–Base Reactions Investigated in the Gas Phase at 300°K

Acid–base reaction	cm^3 molecule^{-1} sec^{-1} k_{forward}	k_{reverse}	K
1. $n\text{-}C_4H_9SH + CH_2NO_2^- \rightleftharpoons CH_3NO_2 + n\text{-}C_4H_9S^-$	>1.6 (−10)	≳2.6 (−11)	>6
2. $CH_3NO_2 + C_5H_5^- \rightleftharpoons C_5H_6 + CH_2NO_2^-$	≳1 (−10)	<1 (−11)	≳10
3. $CH_3NO_2 + CCl_3^- \rightleftharpoons CHCl_3 + CH_2NO_2^-$	≳1 (−10)	≳5 (−12)	≳20
4. $C_5H_6 + CCl_3^- \rightleftharpoons CHCl_3 + C_5H_5^-$	~2 (−11)	≳2 (−11)	≳1
5. $CHCl_3 + CH_3COCH_2^- \rightleftharpoons CH_3COCH_3 + CCl_3^-$	>2 (−10)	<1 (−12)	>200
6. $CHCl_3 + CH_2CN^- \rightleftharpoons CH_3CN + CCl_3^-$	≳1 (−10)	<5 (−12)	>20
7. $CHCl_3 + C_3H_3^{-\,a} \rightleftharpoons C_3H_4 + CCl_3^-$	≳2 (−10)		
8. $CH_3COCH_3 + CH_2CN^- \rightleftharpoons CH_3CN + CH_3COCH_2^-$	≳1 (−10)	≳3 (−11)	≳3
9. $CH_3CN + CHCl_2^- \rightleftharpoons CH_2Cl_2 + CH_2CN^-$	≳2 (−10)		
10. $CH_3CN + CH_3SOCH_2^- \rightleftharpoons CH_3SOCH_3 + CH_2CN^-$	≳2 (−10)	<1 (−11)	>20
11. $CH_3CN + C_2H^- \rightleftharpoons C_2H_2 + CH_2CN^-$	≳1 (−10)		
12. $CH_3CN + C_3H_3^{-\,a} \rightleftharpoons C_3H_4 + CH_2CN^-$	≳5 (−11)		
13. $CH_2Cl_2 + CH_3SOCH_2^- \rightleftharpoons CH_3SOCH_3 + CHCl_2^-$	≳2 (−10)	≳1 (−11)	
14. $CH_2Cl_2 + C_2H^- \rightleftharpoons C_2H_2 + CHCl_2^-$	≳2 (−10)	~3 (−11)	≳6
15. $CH_2Cl_2 + t\text{-}C_4H_9O^- \rightleftharpoons t\text{-}C_4H_9OH + CHCl_2^-$	≳1 (−10)	≳1 (−10)	≳1
16. $CH_2Cl_2 + C_2H_5O^- \rightleftharpoons C_2H_5OH + CHCl_2^-$	≳5 (−11)		
17. $CH_3SOCH_3 + C_2H^- \rightleftharpoons C_2H_2 + CH_3SOCH_2^-$	≳1 (−11)	≳1 (−11)	≳1
18. $CH_3SOCH_3 + C_6H_5CH_2^- \rightleftharpoons C_6H_5CH_3 + CH_3SOCH_2^-$	>5 (−12)	≳1 (−12)	≳5
19. $C_2H_2 + t\text{-}C_4H_9O^- \rightleftharpoons t\text{-}C_4H_9OH + C_2H^-$	1.6 (−10)	≳5 (−11)	≲3
20. $C_2H_2 + i\text{-}C_3H_7O^- \rightleftharpoons i\text{-}C_3H_7OH + C_2H^-$	5.2 (−10)	~5 (−10)	~1
21. $C_2H_2 + C_2H_5O^- \rightleftharpoons C_2H_5OH + C_2H^-$	1.1 (−9)	~1 (−10)	~11
22. $C_2H_2 + CH_3O^- \rightleftharpoons CH_3OH + C_2H^-$	1.3 (−9)	~5 (−11)	~26
23. $C_2H_2 + C_3H_3^- \rightleftharpoons C_3H_4{}^b + C_2H^-$		<1 (−12)	
24. $C_2H_2 + C_6H_5CH_2^- \rightleftharpoons C_6H_5CH_3 + C_2H^-$	~5 (−11)	<1 (−11)	>5
25. $t\text{-}C_4H_9OH + i\text{-}C_3H_7O^- \rightleftharpoons i\text{-}C_3H_7OH + t\text{-}C_4H_9O^-$	≳5 −11)	≳5 (−11)	
26. $t\text{-}C_4H_9OH + C_2H_5O^- \rightleftharpoons C_2H_5OH + t\text{-}C_4H_9O^-$	≳5 (−11)	≳5 (−11)	
27. $t\text{-}C_4H_9OH + CH_3O^- \rightleftharpoons CH_3OH + t\text{-}C_4H_9O^-$	≳5 (−11)	≳5 (−11)	
28. $i\text{-}C_3H_7OH + C_2H_5O^- \rightleftharpoons C_2H_5OH + i\text{-}C_3H_7O^-$	≳5 (−11)	≳5 (−11)	
29. $C_2H_5OH + CH_3O^- \rightleftharpoons CH_3OH + C_2H_5O^-$	≳5 (−11)	≳5 (−11)	
30. $C_2H_5OH + C_6H_5C(CH_3)_2^- \rightleftharpoons C_6H_5CH(CH_3)_2 + C_2H_5O^-$	≳5 (−11)	≲1 (−11)	≳5
31. $C_2H_5OH + C_6H_5CH_2^- \rightleftharpoons C_6H_5CH_3 + C_2H_5O^-$	≳1 (−10)	<5 (−11)	>2
32. $CH_3OH + C_3H_3^{-\,a} \rightleftharpoons C_3H_4{}^b + CH_3O^-$	≳1 (−11)	~5 (−12)	≳2
33. $CH_3OH + C_6H_5C(CH_3)_2^- \rightleftharpoons C_6H_5CH(CH_3)_2 + CH_3O^-$	≳5 (−11)	≳5 (−11)	≳1
34. $CH_3OH + C_6H_5CH_2^- \rightleftharpoons C_6H_5CH_3 + CH_3O^-$	≳5 (−11)	≳5 (−11)	≳1
35. $CH_3OH + C_3H_5^- \rightleftharpoons C_3H_6 + CH_3O^-$	≳5 (−11)	<5 (−12)	>10
36. $C_3H_4{}^b + C_6H_5CH_2^- \rightleftharpoons C_6H_5CH_3 + C_3H_3^{-\,a}$	~6 (−12)	≳5 (−12)	≳1
37. $p\text{-}t\text{-}C_4H_9(C_6H_4)CH_3{}^c + C_6H_5CH_2^- \rightleftharpoons C_6H_5CH_3 + p\text{-}t\text{-}C_4H_9(C_6H_4)CH_2^-$		<5 (−12)	
38. $C_6H_5CH(CH_3)_2 + C_6H_5CH_2^- \rightleftharpoons C_6H_5CH_3 + C_6H_5C(CH_3)_2^-$	~1 (−12)	~5 (−13)	~2
39. $C_6H_5CH(CH_3)_2 + C_6H_5^- \rightleftharpoons C_6H_6 + C_6H_5C(CH_3)_2^-$	~1 (−11)	≳1 (−13)	≳100
40. $C_6H_5CH_3 + C_3H_5^- \rightleftharpoons C_3H_6 + C_6H_5CH_2^-$	~1 (−11)	<1 (−12)	>10
41. $C_6H_5CH_3 + C_6H_5^- \rightleftharpoons C_6H_6 + C_6H_5CH_2^-$	≳5 (−11)		
42. $C_3H_6 + OH^- \rightleftharpoons H_2O + C_3H_5^-$	2.7 (−10)		
43. $H_2O + C_6H_5^- \rightleftharpoons C_6H_6 + OH^-$	≳5 (−11)	<5 (−12)	>10
44. $H_2O + H^- \rightleftharpoons H_2 + OH^-$	≳5 (−11)	<5 (−12)	>10
45. $H_2O + NH_2^- \rightleftharpoons NH_3 + OH^-$	≳5 (−11)	<5 (−12)	>10
46. $H_2O + C_2H_3^- \rightleftharpoons C_2H_4 + OH^-$		≲1 (−12)	
47. $H_2O + CH_3^- \rightleftharpoons CH_4 + OH^-$		≲1 (−12)	
48. $H_2O + (CH_2)_2CH^- \rightleftharpoons (CH_2)_3 + OH^-$		≲3 (−12)	
49. $C_6H_6 + H^- \rightleftharpoons H_2 + C_6H_5^-$	≳5 (−11)	<5 (−12)	>10
50. $C_6H_6 + NH_2^- \rightleftharpoons NH_3 + C_6H_5^-$		≲5 (−12)	
51. $C_6H_6 + CH_3^- \rightleftharpoons CH_4 + C_6H_5^-$		≲5 (−12)	
52. $H_2 + NH_2^- \rightleftharpoons NH_3 + H^-$	≥3.7 (−11)	~4 (−12)	≳10
53. $H_2 + CH_3^- \rightleftharpoons CH_4 + H^-$		≲5 (−12)	
54. $H_2 + (CH_2)_2CH^- \rightleftharpoons (CH_2)_3 + H^-$		≲7 (−12)	
55. $NH_3 + C_2H_3^- \rightleftharpoons C_2H_4 + NH_2^-$		≲1 (−12)	
56. $NH_3 + CH_3^- \rightleftharpoons CH_4 + NH_2^-$		≲5 (−12)	
57. $NH_3 + C_6H_{11}^- \rightleftharpoons C_6H_{12} + NH_2^-$		<1 (−12)	
58. $NH_3 + (CH_2)_2CH^- \rightleftharpoons (CH_2)_3 + NH_2^-$		≲5 (−12)	

[a] $C_3H_3^-$ derived from allene. [b] Allene. [c] The vapor pressure of DMSO at 300°K was too low for the determination of a limit to the rate constant.

peaks are present at m/e 26, 46, and 65, which presumably correspond to the CN^-, NO_2^-, and $C_5H_5^-$ ions. The m/e 121 ion was observed to be chemically coupled to the m/e 60 ion. With addition of increasing amounts of nitromethane to the helium afterglow, the intensity of the m/e 121 ion increased at the expense of the m/e 60 ion. This result was taken as evidence that the m/e 121 ion was the $CH_2NO_2^-$ ion solvated with one molecule of CH_3NO_2 and that this solvated ion was

formed via the three-body association reaction 6. A number of such solvation processes were observed in

$$CH_2NO_2^- + CH_3NO_2 + He \rightleftharpoons CH_2NO_2^- \cdot CH_3NO_2 + He \quad (6)$$

the course of these studies. However, no further investigations were made into the nature of these processes at this time. According to Figure 2, the addition of n-butyl mercaptan into the reaction region of the flow system led to a sharp decrease in both m/e

60 and 121 ion intensity and a simultaneous increase in the intensity of the m/e 89 ion. This is demonstrated by the mass spectra labeled 2 and 3. Spectrum 3 shows that the m/e 60 ion intensity has decreased by more than a factor of 10 without any significant increase in the total pressure in the reaction region as a result of the addition of n-butyl mercaptan, i.e., $\Delta P \lesssim 0.0001$ Torr. This result provides evidence that the proton-

$$CH_2NO_2^- + n\text{-}C_4H_9SH \longrightarrow n\text{-}C_4H_9S^- + CH_3NO_2 \quad (7a)$$
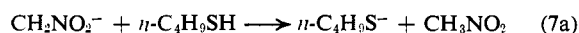
transfer reaction proceeds rapidly with a rate constant which can be calculated from the known reaction time, 4.6 msec, as $\gtrsim 1.6 \times 10^{-10}\,cm^3\,molecule^{-1}\,sec^{-1}$. Figure 3 displays the mass spectral scans taken at various extents of the backward reaction, i.e., the reaction of n-$C_4H_9S^-$ with nitromethane. The mass spectrum labeled 1 illustrates that the n-$C_4H_9S^-$ ion is easily established as the dominant negative ion in the flowing afterglow. The spectra labeled 2 and 3 result from the addition of nitromethane. The observed masses are easily identified. Ions with m/e 60, 121, 150, and 182 appear with small additions of CH_3NO_2 at the expense of the m/e 89 ion, which decreases significantly in intensity. A sequence of three-body solvation reactions initiated by the proton-transfer reaction 7b and

$$n\text{-}C_4H_9S^- + CH_3NO_2 \longrightarrow CH_2NO_2^- + C_4H_9SH \quad (7b)$$
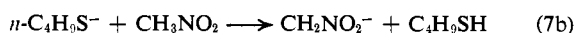
leading to the formation of $CH_2NO_2^- \cdot CH_3NO_2$ and $CH_2NO_2^- \cdot 2CH_3NO_2$ are believed to be responsible for the observation of the m/e 60, 121, and 182 ions, respectively. The ion with m/e 150 is believed to correspond to the n-$C_4H_9S^-$ ion solvated with one molecule of nitromethane. The formation of this ion is a result of associative collisions between nitromethane molecules and mercaptide ions of insufficient energy to undergo the endothermic proton-transfer reaction 7b. There was no evidence for the occurrence of a competing reaction channel of type 8 corresponding

$$n\text{-}C_4H_9S^- + CH_3NO_2 \longrightarrow NO_2^- + n\text{-}C_4H_9SCH_3 \quad (8)$$

to nucleophilic substitution. A definite pressure increase of 0.0006 Torr was registered for an order of magnitude decay in the n-$C_4H_9S^-$ ion signal with addition of nitromethane. This observation led to an upper limit estimate of the rate constant for reaction 7b of $2.6 \times 10^{-11}\,cm^3\,molecule^{-1}\,sec^{-1}$. This results in a limit to the equilibrium constant for reaction 1 in Table I of $K > 6$. Analogous studies yielded the remaining kinetic data listed in Table I. Reactions 42, 46, and 47 have been reported previously in conjunction with studies of the gas-phase reactivity of hydroxide ion toward unsaturated and saturated hydrocarbons.[4a,8] Reactions 44, 45, and 52 were recently reported in connection with the determination of the relative acidity of H_2O, H_2, and NH_3 in the gas phase.[4b] Finally, reactions 19–22, 25, 28, and 29 were also reported recently in a comparative study of the acidities of the alcohols.[4c]

Discussion

We are primarily concerned in this study with the application of the flowing afterglow technique to the determination of relative acidity in the gas phase from a study of the kinetics of proton-transfer reactions of

(8) D. K. Bohme and F. C. Fehsenfeld, Can. J. Chem., 47, 2717 (1969).

type 1. Acidity or acid strength can be expressed either in terms of the proton affinity of the conjugate base, e.g., PA(A⁻), or in terms of the acid dissociation constant, e.g., pK_a(AH). The former expression is often favored among gas-phase chemists, whereas the latter expression is most familiar to solution chemists.

The proton affinity of a negative ion A⁻, PA(A⁻), is defined as the negative standard enthalpy change at 298°K for the reaction $A^- + H^+ \rightarrow AH$. Accordingly, the standard enthalpy change for the proton-transfer reaction 1, proceeding at room temperature, is a measure of the relative proton affinity of the conjugate bases A⁻ and B⁻. If the standard enthalpy change, $\Delta H°$, is approximately equal to the standard free energy change, $\Delta G°$, then

$$\Delta G° \approx \Delta H° = PA(B^-) - PA(A^-) \quad (9)$$

and the magnitude of $\Delta G°$ becomes a quantitative measure of the difference in the proton affinity of the two conjugate bases. $\Delta G°$ can be evaluated from rate constant data. Briefly, if k_1 and k_2 represent the rate constants for the forward and reverse proton transfer, respectively, then, according to classical thermodynamics, the standard free energy change, $\Delta G°$, accompanying the process can be related to these rate constants by eq 10. Equation 10 is strictly applicable

$$\Delta G° = -RT \ln k_1/k_2 \quad (10)$$

only if the rate constants are measured under conditions where the translational and internal energy distributions of the respective reactants are Maxwell–Boltzmann.

The strength of an acid in terms of its pK_a value is normally formulated on the basis of proton-transfer reactions proceeding in solution. The pK_a is defined by eq 11 in terms of the thermodynamic equilibrium

$$pK_a = -\log K'_{eq}[H_2O] \quad (11)$$

constant, K'_{eq} of the proton-transfer reaction 12 pro-

$$AH + H_2O \rightleftharpoons A^- + H_3O^- \quad (12)$$
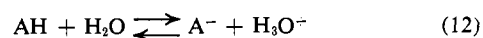
ceeding in aqueous solution (we have chosen water as the standard base). We can also adopt this definition of pK_a in the gas phase. However, since reaction 12 does not normally proceed to any detectable extent in the gas phase, an experimental determination of K_{eq}, and thus pK_a, is prohibited in the gas phase. Nevertheless, differences in gas phase pK_a values, which are related to the thermodynamic equilibrium constant, K_{eq}, of the proton-transfer reaction 1 by eq 13, are now becoming quite accessible to gas-phase experiments.

$$\Delta pK_a \equiv pK_a(AH) - pK_a(BH) = \log K_{eq} \quad (13)$$

According to either of the two definitions of acidity given above, the relative acidity of two acids can be established from kinetic data on proton-transfer reactions of type 1. A knowledge of the absolute magnitude of the rate constants for the forward and reverse directions of proton transfer yields a quantitative measure of the difference in the acid strength of two acids. A knowledge of only the preferred direction of proton transfer, i.e., a knowledge of only the relative magnitude of the forward and reverse rate constants,

yields a qualitative measure of the difference in the acidity of two acids. In both instances the rate constants must pertain to reactions in which the translational and internal energy distributions of the reactants are Maxwell–Boltzmann. All of the kinetic data listed in Table I were obtained in a large excess of helium carrier gas. After their initial formation, the reactant ions were allowed to undergo many thousands of collisions with the carrier gas before entering the reaction region in which we expect them to be thermalized. The helium carrier gas and the neutral reactant vapors are, of course, already in thermal equilibrium upon addition into the flowing afterglow tube. Consequently we expect that the energy distributions of the reactants in question are Maxwell–Boltzmann. The ratio of the rate constant for the forward direction of proton transfer to the rate constant for the reverse direction can then be taken to be equal to the thermodynamic equilibrium constant.

Due to the difficulties encountered in these experiments in the measurement of the concentrations of many of the neutral reactants in the range of concentrations of interest, the studies reported in this paper are, for the main, restricted to the determination of limits to the rate constants in question. Consequently only a knowledge of the preferred direction of proton transfer was accessible in the majority of the investigations and only the relative acidity could be established. The following gas-phase acidity order (in order of decreasing acidity) can be deduced from the kinetic data given in Table I: $n\text{-}C_4H_9SH > CH_3NO_2 > C_5H_6 \gtrsim CHCl_3 > CH_3COCH_3 > CH_3CN > CH_2Cl_2$, $CH_3SOCH_3 \gtrsim C_2H_2$, $tert\text{-}C_4H_9OH$, $i\text{-}C_3H_7OH > C_2H_5OH > CH_3OH > C_3H_4$, $C_6H_5CH(CH_3)_2 > C_6H_5CH_3 > C_3H_6 > H_2O > C_6H_6 > H_2 > NH_3 > C_2H_4$, C_6H_{12}, $(CH_2)_3$, CH_4. In the majority of the cases we were able to establish the relative acidity of two adjacent acids from a direct determination of the preferred direction of proton transfer between one of the acids and the conjugate base of the adjacent acid. This was, however, not always possible, especially in the case of the alcohols since it was observed that proton-transfer reactions between the selected alcohol molecules and alkoxide ions (reactions 25–29 in Table I) were quite rapid in both directions, $k \gtrsim 5 \times 10^{-11}$ cm^3 molecule^{-1} sec^{-1}. This result is simply a manifestation of the small differences in the acid strengths of these alcohols in the gas phase. On the basis of the kinetic data for reactions 25–29 given in Table I and accepting the acidity order[9] $tert\text{-}C_4H_9OH > i\text{-}C_3H_7OH > C_2H_5OH > CH_3OH$, we estimate that $\Delta G°_{300}$ is of the order of 0–3 kcal/mol for these reactions. This amounts to a difference of, at most, 2 pK_a units between any two of the alcohols under consideration. In order to make this estimate we must assume that the rate constant for the forward direction of proton transfer cannot exceed 5×10^{-9} cm^3 molecule^{-1} sec^{-1}.[10] In spite of our inability to compare the acidity of the various alcohols directly, we did

succeed in comparing their acid strengths indirectly by measuring their tendency to transfer a proton to the same base, namely C_2H^-, which is the anion derived by proton abstraction from acetylene. The kinetic data given in Table I for reactions 19–22 indicate that, in the gas phase, p$K_a(C_2H_2) \simeq$ p$K_a(i\text{-}C_3H_7OH)$, p$K_a(i\text{-}C_3H_7OH) \simeq$ p$K_a(C_2H_5OH) - 1$, and p$K_a(C_2H_5OH) \simeq$ p$K_a(CH_3OH) - 0.5$. These results are consistent with the estimates of limits to ΔpK_a made above from the kinetic data for reactions 25–29 in Table I.

A number of the reactions listed in Table I have been investigated in the gas phase by other workers employing different experimental techniques. Of principal interest and relevance is the work of Brauman and Blair who employed the pulsed double resonance mode in an ion cyclotron resonance (icr) spectrometer to determine relative gas-phase acidities.[2] Operation in this mode and the interpretation applied by these authors to their recorded observations has led to the following orders of ability to transfer a proton: $tert\text{-}C_4H_9OH > i\text{-}C_3H_7OH > C_2H_5OH > CH_3OH > H_2O$, $C_2H_5OH > C_6H_5CH_3 > CH_3OH$, and $CH_3NO_2 > CH_3COCH_3 > tert\text{-}C_4H_9OH$. These orders were based simply on the occurrence or nonoccurrence of selected proton-transfer reactions in an icr cell. For example, the double resonance results reported for the forward and reverse proton-transfer reactions 25, 28, 29, and 34 in Table I and the reverse proton-transfer reaction 31 in Table I indicate occurrence in the forward direction for the former series of reactions and nonoccurrence in the reverse direction for the latter reaction. Brauman and Blair feel that this observed order of ability to transfer a proton in the icr cell is an accurate reflection of the sign of $\Delta G°$[12] and thus represents a true gas-phase acidity order. The present results are in agreement with the acidity sequences first established by Brauman and Blair with the sole exception of the position assigned to toluene. We cannot base the position of toluene in our acidity order solely on the kinetic results for reaction 34 in Table I which, within the experimental error associated with the measurement of concentrations, are not in disagreement with the results of Brauman and Blair. However, we feel that our results for reaction 34 together with the additional results for the kinetics of reactions 38 and 33 as well as for reactions 36 and 32 are more consistent with the position ascribed to toluene in our sequence of acidity.

Our kinetic results do not preclude a difference in the acidity of methanol and toluene of only a few tenths of a pK_a unit. It is therefore conceivable that only a small amount of excitation of reactants could reverse this acidity order. Consequently one needs to be very concerned about the average energies and energy distributions of the reacting species when trying to establish relative acidity on the basis of kinetic observations of this type. In these experiments we rely on the many tens of thousand collisions which the anions undergo before reaction to completely thermalize them. The ions undergo at most approximately ten collisions before reaction under the typical operating pressures of the early icr experiments. Consequently the possible interference by excited (both electronic

(9) Although we did not conclusively establish that $tert\text{-}C_4H_9OH$ is a stronger acid than $i\text{-}C_3H_7OH$ in the gas phase, we assume this to be true on the basis of the results of Brauman and Blair (ref 2).

(10) A maximum theoretical collision rate constant can be calculated on the assumption that the dipole "locks in" as the ion approaches (ref 11). It was taken to be approximately equal to 5×10^{-9} cm^3 molecule^{-1} sec^{-1} for all of the alcohol reactions in question.

(11) D. K. Bohme and L. B. Young, J. Amer. Chem. Soc., 92, 7354 (1970).

(12) A temperature was not assigned by Brauman and Blair to the standard free energy change, $\Delta G°$.

and vibrational) states of the anions is likely to be more severe in these investigations. We assume here that significant perturbations due to the presence of excited states are absent in the flowing afterglow results so that the measured acidity order reflects the ground-state acidity order. This assumption is partially justified by the internal consistency of the experimental results.

Comparison with Solution. The order of acid strength determined in the gas phase is an intrinsic acidity order which truly reflects intrinsic structure-reactivity relationships.[1] The extent to which this may also be true in solution has long been a point of controversy among solution chemists,[13] although it has been recognized for many years that the acidity of uncharged acids can be very sensitive to the nature of the solvent.[14,15] The recent work of Brauman and Blair[2] first demonstrated that truly intrinsic acidity orders have now become accessible to experiment and that these orders can be valuable both in the correlation of structure and reactivity on a molecular level, and, when compared with solution, in the evaluation of the nature of bulk solvent effects.

The difference in the acidity of two acids in solution, i.e., the value of ΔpK_a in solution, is expected to be most sensitive to solvation when the absolute magnitude of the intrinsic value of ΔpK_a is small. This is borne out by the present experimental results. For example, we have shown that $pK_a(C_2H_5OH) - pK_a(i\text{-}C_3H_7OH) \equiv \Delta pK_a{}^i \simeq 1$ and that $pK_a(C_2H_5OH) - pK_a(tert\text{-}C_4H_9OH) \equiv \Delta pK_a{}^t \gtrsim 1$ in the gas phase at 300°K. Solution measurements suggest that $\Delta pK_a{}^i = 0$ and $\Delta pK_a{}^t = -1$ in benzene[16] at room temperature and that $\Delta pK_a{}^t = 0$ in dimethyl sulfoxide solution[17] at room temperature. Thus, both the absolute magnitude and the sign of ΔpK_a can change in going from the gas phase to, in this case, benzene or dimethyl sulfoxide solution. A further illustration can be found with reference to the early work of Unmack[18] on the acid-base equilibrium 14. Despite the limitation of the

$$OH^- + CH_3OH \rightleftharpoons CH_3O^- + H_2O \qquad (14)$$

techniques and analyses employed by Unmack to derive a thermodynamic equilibrium constant, K'_{eq}, for reaction 14 in solution, his experimental results indicate that K'_{eq} at 291°K could be greater than or less than 1 depending on whether the investigations were carried out in an excess of water or methyl alcohol, i.e., a change in sign of ΔpK_a in going from water to methyl alcohol as solvent. In the gas phase we find that $K_{eq} > 1$ for reaction 14 at 300°K.

Water and the alcohols are oxygen acids. The shift in the value of ΔpK_a between oxygen and carbon acids can be much more dramatic. Thus, whereas $pK_a(H_2O) - pK_a(DMSO) \gtrsim 2$ in the gas phase at 300°K, water is considerably more acidic (by nearly 4 pK_a units) than dimethyl sulfoxide in dimethyl sulfoxide solution.[17] In aqueous solution $pK_a(H_2O) - pK_a(\text{acetone}) = -4$ and $pK_a(H_2O) - pK_a(CH_3CN) = -9$

at room temperature.[19] Our gas-phase experiments indicate that $pK_a(H_2O) - pK_a(\text{acetone}) \gtrsim 3.2$ and that $pK_a(H_2O) - pK_a(CH_3CN) \gtrsim 2.7$. This latter result indicates a change in the value of ΔpK_a of more than 11 pK_a units in going from the gas phase to aqueous solution! This means that the equilibrium constant for the acid-base equilibrium 15 changes by at least a

$$OH^- + CH_3CN \rightleftharpoons CH_2CN^- + H_2O \qquad (15)$$
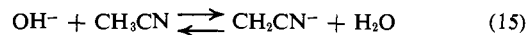
factor of 5×10^{11} and that the standard free energy change for this reaction proceeding in aqueous solution is at least 16 kcal/mol more positive than it is in the gas phase.

Changes in the sign of ΔpK_a in going from the gas phase to solution can also be identified for pairs of carbon acids. In the following comparisons the values of ΔpK_a in solution were derived from the McEwen-Streitwieser-Applequist-Dessy (MSAD) pK_a scale. According to the present kinetic data, $pK_a(\text{toluene}) - pK_a(\text{cumene}) \cong 0.3$ in the gas phase, whereas $\Delta pK_a = -2$ in solution. $pK_a(\text{benzene}) - pK_a(\text{cumene}) \gtrsim 2.3$ in the gas phase and 0 in solution. $pK_a(\text{propene}) - pK_a(\text{toluene}) \gtrsim 1$ in the gas phase and ~ 0.5 in solution. $pK_a(\text{benzene}) - pK_a(\text{propene}) \gtrsim 1$ in the gas phase and 1.5 in solution. $pK_a(\text{ethylene}) - pK_a(\text{benzene}) \gtrsim 2$ in the gas phase and ~ 0.5 in solution.

Kinetics of Proton Transfer. The majority of the absolute values and limiting values for the forward rate constants for proton transfer listed in Table I are in accord with a moderately high reactivity (reaction probability $\gtrsim 0.01$) for the conjugate bases in the gas phase at 300°K. Furthermore, there again seems to be some correlation of the reactivity of the anions with the nature of the distribution of their charge.[11] For example, in the series of acid-base reactions between alkoxide ions and acetylene (reactions 19–22 in Table I), the anion reactivity is highest for the least charge-delocalized ion, CH_3O^-. Also the benzyl anion, a delocalized system, generally shows a low reactivity.

The reactions 38 and 39 in Table I are of particular interest. As was the case for the reactions with methyl chloride, the phenyl carbanion is considerably more reactive than the benzyl carbanion toward proton abstraction from cumene. However, even the low reactivity of the phenyl carbanion (reaction probability $\sim 2 \times 10^{-3}$) is unusually low (cf. reaction 41 in Table I). We regard this result as providing evidence for the role of steric hindrance in these two ion–molecule reactions proceeding in the gas phase. The extra-low reactivity of the benzyl anion and the low reactivity of the phenyl anion toward removal of the most acidic proton in cumene are therefore partially attributed to the steric hindrance by the two methyl groups.

Thermochemical Results. The identification of the preferred direction of proton transfer in reaction 1 as the exothermic (or thermoneutral) direction allows the determination of chemically useful limiting values for electron and proton affinities. For example, if reaction 1 is exothermic (or thermoneutral) in the direction as written, then $PA(B^-) \leq PA(A^-)$ and $EA(B) \geq EA(A) D + (B - H) - D(A - H)$. Thus, a knowledge

(13) See, for example: C. D. Ritchie and R. E. Uschold, *J. Amer. Chem. Soc.*, **90**, 2821 (1968).
(14) E. Grunwald and E. Price, *ibid.*, **86**, 4517 (1964).
(15) B. W. Clare, D. Cook, E. C. F. Ko, Y. C. Mac, and A. J. Parker, *ibid.*, **88**, 1911 (1966).
(16) W. K. McEwen, *ibid.*, **58**, 1124 (1936).
(17) E. C. Steiner and J. M. Gilbert, *ibid.*, **87**, 382 (1965).
(18) A. Unmack, *Z. Phys. Chem.*, **133**, 45 (1928).

(19) R. G. Pearson and R. L. Dillon, *J. Amer. Chem. Soc.*, **75**, 2439 (1953).

Table II. Thermochemical Data[a]

XH	D_{298}(X–H)	EA(X) This work	EA(X) Lit. values	PA(X⁻)
n-C₄H₉SH	4.2[b]	>1.5		<16.3
CHCl₃	4.15[c]	>1.45	1.22[d]	<16.3
CH₃COCH₃	4.03[e]	>1.33		<16.3
CH₃CN	3.73[c]	>1.13		<16.3
C₂H₂	4.9[f]	2.2	2.70[d]	≤16.3
t-C₄H₉OH	4.47[c]	≥1.77		≤16.3
i-C₃H₇OH	4.47[c]	1.77[g]	0.67[d]	16.3
C₂H₅OH	4.43[c]	1.68[g]	0.59[d]	16.35
CH₃OH	4.43[c]	1.15–1.68	0.38[d]	16.35–16.88
C₆H₅CH₃	3.69[c]	0.4–0.9	0.8,[d] 0.69[h]	16.35–16.88
C₃H₆	3.69[c]	0.4–0.9	2.1,[d] 0.24,[h] 0.52[i]	16.35–16.88
	3.86[e]	0.6–1.1		
H₂O	5.11[j]	1.83[k]		16.88
C₆H₆	4.86[e]	1.2–1.6	2.3[d]	16.9–17.3
H₂	4.48[l]	0.75[m]		17.33
NH₃	4.73[n]	<1.0	1.12,[d] 0.74,[o] 0.76[p]	>17.3
CH₄	4.51[e]	<0.78	1.05–1.08[d]	>17.3
c-C₃H₆	4.38[c]	<0.65		>17.3
c-C₆H₁₂	4.07[c]	<0.34		>17.3

[a] All values in eV. [b] We assume that D(n-C₄H₉S—H) $\cong$ D(C₂H₅S—H) = 4.2 eV: C. T. Mortimer, "Reaction Heats and Bond Strengths," Pergamon Press, New York, N. Y., 1962. [c] J. A. Kerr, Chem. Rev., 66, 465 (1966). [d] F. M. Page and G. C. Goode, "Negative Ions and the Magnetron," Wiley-Interscience, New York, N. Y., 1969. [e] D. M. Golden and S. W. Benson, Chem. Rev., 69, 125 (1969). [f] B. E. Knox and H. B. Palmer, ibid., 61, 247 (1961). [g] J. M. Williams and W. H. Hamill, J. Chem. Phys., 49, 4467 (1968). [h] N. S. Hush and J. A. Pople, Trans. Faraday Soc., 51, 600 (1955). [i] J. R. Hoyland and L. Goodman, J. Chem. Phys., 36, 21 (1962). [j] G. Herzberg, "Molecular Spectra and Molecular Structure," Vol. III, "Electronic Spectra and Electronic Structure of Polyatomic Molecules," Van Nostrand, New York, N. Y., 1966. [k] L. M. Branscomb, Phys. Rev., 148, 11 (1966). [l] G. Herzberg, "Molecular Spectra and Molecular Structure," Vol. I, "Spectra of Diatomic Molecules," Van Nostrand, New York, N. Y., 1953. [m] C. L. Pekeris, Phys. Rev., 126, 1470 (1962). [n] S. W. Benson, private communication. [o] K. C. Smyth, R. T. McIver, J. I. Brauman, and R. W. Wallace, J. Chem. Phys., 54, 2758 (1971). [p] D. Feldmann, Z. Naturforsch. A, 26, 1100 (1971).

of the sign of $\Delta H°$ and one proton affinity allows a limit to be set on the other proton affinity. Also a knowledge of the sign of $\Delta H°$ together with two bond dissociation energies and one electron affinity allows a limit to be set on the other electron affinity. Table II includes a summary of the limiting values for electron and proton affinities which can be determined in the manner just described from the acidity order given earlier. We assume here that the acidity order is identical with the proton affinity order of the corresponding conjugate bases; i.e., we assume that the sign of $\Delta G°$ is the same as the sign of $\Delta H°$ in all of the reactions investigated. The required bond dissociation energy data were available in most instances. The values for the electron affinity of H, OH, C₂H₅O, and i-C₃H₇O were considered to be well established and were used as reference values. The derived limits to electron affinity are compared in Table II with the electron affinity data currently available in the literature. The bulk of the electron affinity values available for comparison were determined experimentally by Page and coworkers who employed the magnetron technique developed by them. In general there is poor agreement between the values determined with the magnetron technique and the limiting values determined from the

present investigations of the kinetics of proton transfer reactions proceeding in the gas phase at 300°K.

Our limit for EA(CH₃) given in Table II supersedes, but is consistent with, that determined earlier on the basis of the failure to observe proton transfer from CH₄ to OH⁻ at 300°K.[8] The high value for EA(CH₃) determined by Page would make the proton abstraction from CH₄ by H⁻ and NH₂⁻ exothermic for ground state reactants by several tenths of an electron volt. The failure to observe proton transfer in these cases in the flowing afterglow at 300°K indicates otherwise. In fact, the abstraction of a proton from saturated hydrocarbon molecules in general by ion–molecule reaction in the gas phase at 300°K using a variety of anions as bases has, as yet, not been detected by us.

The kinetic results given in Table I suggest, as summarized in Table II, that the true values for the electron affinity of NH₂, C₆H₅, C₃H₅, and C₂H should be lower than those given by Page and that the actual values for the electron affinity of CH₃O and CCl₃ should be higher.

While this manuscript was in preparation two new experimental measurements of the electron affinity of NH₂ were reported. These have been included in Table II.